

Sub-rapid Solidification Study of Silicon Steel by Using Dip Test Technique



Hairui Qian and Wanlin Wang

Abstract Dip test technique has been used for the study of sub-rapid solidification (cooling rate ranges from 100 °C/s up to 1000 °C/s) of molten steel to effectively simulate the thermophysical phenomena during strip casting process due to its convenient and online observation advantages. In this study, a 6.5 wt% Si electric steel strip was produced by an improved dip test apparatus, which has been developed for the research of interfacial heat transfer and microstructure of strip casting steels. The heat transfer rates were calculated by the inverse heat conduction program (IHCP). The analysis of solidification microstructure and second phase precipitation was also carried out by scanning electron microscope (SEM) and transmission electron microscope (TEM). The results showed that the maximum heat flux could be up to 8.2 MW/m², and only a very small amount of MnS (0.5 μm) and AlN (2 μm) precipitates were found in the as-cast strip while nano-size MnS (~50 nm) and TiN (50–200 nm) precipitates were observed with subsequent heat treatment, after which the magnetic properties were also significantly improved.

Keywords Dip test technique · Sub-rapid solidification · Second phase precipitation

Introduction

Silicon steel is widely used in the manufacture of various motors, generator cores, etc., which is an important soft magnetic material in the power, electronics, military, and civil industries [1–3]. Strip casting is a novel steel sheet production technique in which liquid steel is directly solidified onto the twin-cooling mold [4, 5]. Strip casting breaks through the limits of silicon content in traditional silicon steel [6, 7],

H. Qian · W. Wang (✉)

School of Metallurgy and Environment, Central South University, 410083 Changsha, China
e-mail: wanlin.wang@gmail.com

National Center for International Research of Clean Metallurgy, Central South University, 410083 Changsha, China

and the increase of silicon content could significantly reduce the core loss and almost avoid the magnetostriction when the silicon content reaches 6.5 wt% [8].

In strip casting, the heat transfer between the melt and substrate has been determined by its interfacial behavior and the nucleation and growth of initial shell [9], which significantly influences its product performance. Many researches have been carried out on the heat transfer behavior during the solidification in strip casting. Droplet technique and dip test apparatus are effective methods for simulating strip casting process in laboratory [10–14]. The dip test apparatus was designed by Strezov, which approximated the initial contact conditions of a twin roll caster by immersing copper substrates into the molten steel, and then the interfacial heat transfer and the effect of oxide films that naturally deposited on substrate surface on the heat transfer behavior have been studied [15, 16]. Second phase precipitates like AlN and MnS have been proved to have significant relations with the magnetic properties of silicon steel [17, 18]. The existence of precipitates leads to the internal stress and grain boundary pinning during recrystallization [17]. With the proper process to control precipitations and grain texture, strip casting is a promising technique to produce electrical steels.

In this study, 6.5 wt% Si electric steel strips were produced through an improved dip test apparatus, which has been developed at Central South University for the research of interfacial heat transfer and microstructure of strip casting steels.

Experimental Apparatus and Procedure

5 kg experimental raw materials with the major compositions in Table 1 were used in this study, and they were composed of industrial pure iron, ferrosilicon, and electrolytic manganese. The raw materials were polished with abrasive paper and then cleaned in ethanol with ultrasonic agitation prior to dip test experiment so that the oxidized surface layer was removed.

A schematic of the dip test technique is given in Fig. 1. The raw materials were charged into magnesium oxide crucible, which was surrounded by induction coils. The oxygen partial pressure was controlled accurately at 10^{-5} atm. The raw materials were heated in a high-frequency induction furnace. The real-time temperature was measured by an infrared pyrometer installed above a quartz observation window, and a PID device was used to obtain the temperature information and adjust the heating power to achieve a certain superheat (80 °C) of the molten steel. The linear motor loaded with the water-cooling copper mold was set to drop at a speed of 0.7 m/s. The copper mold immersed in the molten steel for 150 ms and then quickly

Table 1 Composition of designed silicon steel

C	Si	Mn	Al	P	S	Ti	Fe
0.003	6.5	1.0	0.040	0.005	0.003	TRACE	Bal.

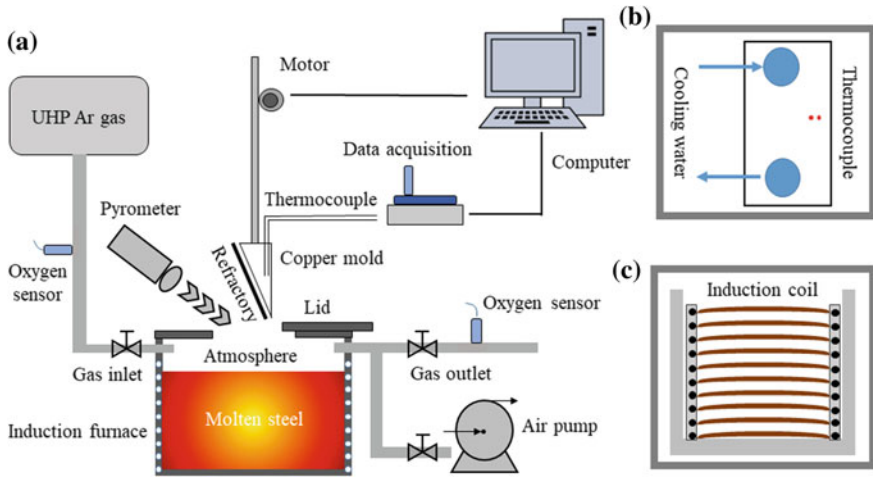


Fig. 1 Schematic illustration of the dip test technique **a** schematic diagram of the dip test technique; **b** designed copper mold; **c** induction coil

returned to the original position. Two high-frequency thermocouples were installed 1 and 3 mm vertically away from the surface of copper mold. Temperature signals during the immerse period were received and transmitted to a computer, and finally, a thin strip about 40 mm * 30 mm, 1 mm in thickness is formed on the surface of the copper mold. The schematic diagram of dip test experimental process is shown in Fig. 2.

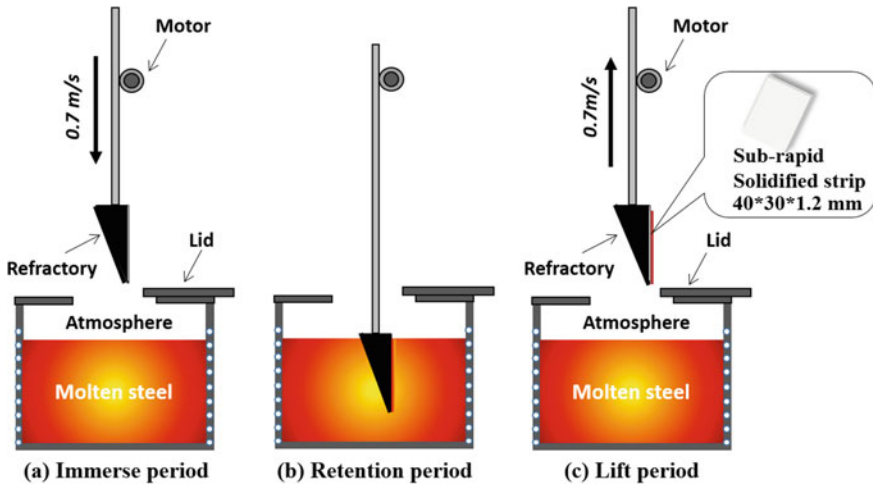


Fig. 2 Schematic diagram of dip test experimental process **a** immerse period; **b** retention period; **c** lift period

Results and Discussion

Interfacial Heat Transfer

The real-time heat transfer behavior of the sub-rapid solidification could be measured by the installed thermocouples, and they are plotted versus time as shown in Fig. 3a. It could be observed that the No. 1 thermocouple rises up instantaneously and reaches the highest value quickly within 0.2 s during the time when the copper substrate contacts with the molten steel and starts initial solidification, then the temperature decreases slowly due to the increase of initial shell that introduces a higher thermal resistance. Finally, the temperature increases continuously due to the continuous heating of the melt bath. However, the temperature of No. 2 increases relatively slowly during the test. Figure 3b shows the interfacial heat flux over time calculated by IHCP [13] from Fig. 3a and the total heat removed during initial solidification is obtained by integrating the heat flux over time. It shows that the heat flux reaches a maximum value of 8.2 MW/m^2 at 0.25 s and then gradually goes down to 2.1 MW/m^2 . The amount of the removed heat increases to 4500 kJ/m^2 in the first 1.1 s. It could be explained that the heat flux picks up very quickly in the first 0.25 s, when the copper mold initially contacts with molten steel and starts initial solidification, then it goes down during the following time with the formation of solidified shell, which causes the formation of air gap leading to the increase of interfacial thermal resistance.

The Solidification Microstructure

The cross section of the as-cast strip could be observed under the optical microscope as shown in Fig. 4a. The results suggest that the microstructure of as-cast silicon steel strip consists of dominant large-size columnar grains along the heat transfer

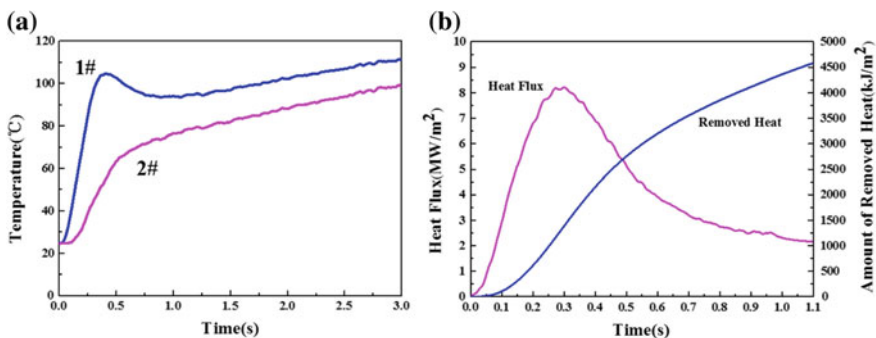


Fig. 3. Heat transfer behavior during sub-rapid solidification **a** the responding temperatures versus time and **b** the calculated interfacial heat flux and the amount of heat removed versus time

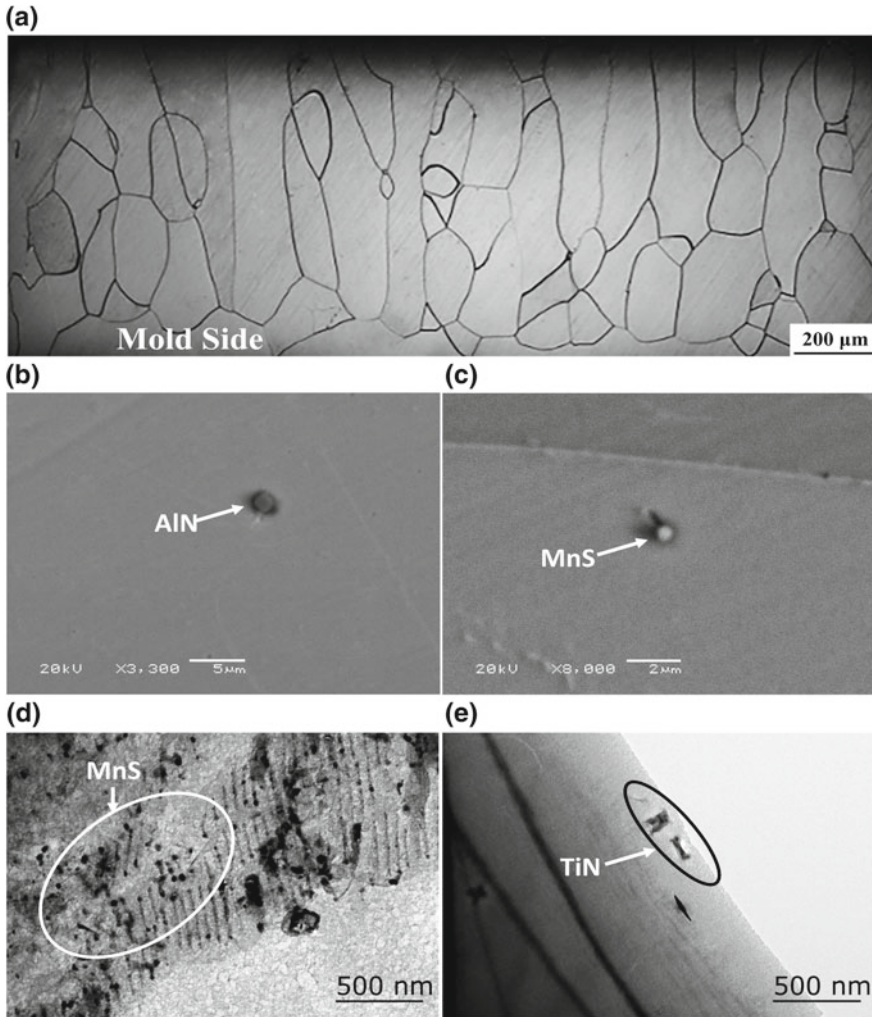


Fig. 4 Microstructure of as-cast strip and precipitation of AlN, MnS, and TiN in silicon steel by dip test **a** Microstructure of as-cast thin strip by dip test; **b** and **c** precipitation of AlN and MnS in as-cast strip; **d** and **e** precipitation of MnS and TiN after heat treatment

direction and a small quantity of equiaxed grains formed at the mold side due to the large cooling rate.

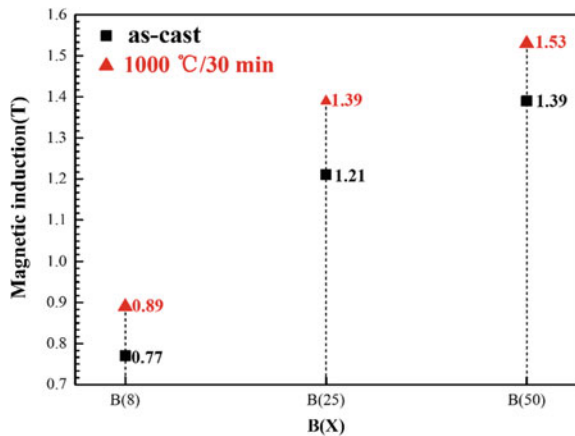
The morphology and dimension of precipitates in as-cast silicon steel strips and heat-treated strips were characterized by scanning electron microscope (SEM) and transmission electron microscope (TEM). Only very few micron size precipitates exist in the as-cast strip (Fig. 4b, c), that has been indicated as AlN and MnS through energy dispersive spectrometer (EDS) analysis. Both AlN and MnS precipitates presented a round shape with a dimension of 2 μm and 0.5 μm, respectively. In strip

casting, the formation of second phase precipitates is inhibited due to the sub-rapid solidification rate, whose cooling rate ranges from 100 °C/s up to 1000 °C/s and the total solidification time is within 0.3 s. Therefore, these alloying elements would be finely dispersed in the Fe matrix. Considering the theoretical precipitation temperature of AlN (~1512 °C) and MnS (~1328 °C) [19, 20], AlN precipitates are supposed to nucleate before sub-rapid solidification, and MnS precipitates subsequently. According to the TEM observation presented in Fig. 4d, e, we could find quantities of precipitates of MnS and TiN formed within the grain, which could not be found in the as-cast strip, due to the heat treatment (1000 °C for 30 min). The size of MnS precipitates is about ~50 nm and 50–200 nm for rectangular AlN precipitates.

Magnetic Induction

Figure 5 shows the magnetic induction of the as-cast strip and the heat-treated strip by vibrating sample magnetometer (VSM). The magnetic induction of as-cast strip at B(8), B(25), and B(50) are 0.77 T, 1.21 T, and 1.39 T, respectively, and they approach to 0.89 T, 1.39 T, and 1.53 T for the heat-treated strip annealed at 1000 °C for 30 min. Compared with the as-cast strip, the magnetic induction performance of the heat-treated strip has been improved considerably. It could be inferred that large amounts of dislocations and defects would remain in as-cast strips when sub-rapid solidification occurs, which would obstruct the movement of magnetic domains, leading to a bad magnetic induction. Thus, the heat treatment is necessary to be carried out to eliminate these dislocations and defects; consequently, the magnetic induction performance is improved as expected.

Fig. 5 Magnetic induction of silicon steel strips before and after heat treatment at 1000 °C for 30 min



Conclusions

The dip test technique has been further developed for the research of interfacial heat transfer and microstructure of strip casting steels. The main conclusions are summarized as follows:

- (1) The improved dip test technique could precisely study the interfacial heat transfer behavior of the sub-rapid solidification for the designed silicon steel, during which the maximum heat flux could be up to 8.2 MW/m^2 .
- (2) SEM and TEM observation results showed that only a very small amount of micron size of MnS ($0.5 \mu\text{m}$) and AlN ($2 \mu\text{m}$) precipitates were found in as-cast strip, while nano-size MnS ($\sim 50 \text{ nm}$) and TiN ($50\text{--}200 \text{ nm}$) precipitates were observed with subsequent heat treatment ($1000 \text{ }^\circ\text{C}/30 \text{ min}$), after which the magnetic induction performance was improved due to the reduction of dislocations and defects.

References

1. Takashima M, Komatsubara M, Morito N (1997) $\{001\} \langle 210 \rangle$ texture development by two-stage cold rolling method in non-oriented electrical steel. *ISIJ Int* 37:1263–1268
2. Xia ZS, Kang YL, Wang QL (2008) Developments in the production of grain-oriented electrical steel. *J Magn Magn Mater* 320:3229–3233
3. Takahashi N, Suga Y, Kobayashi H (1996) Recent developments in grain-oriented silicon-steel. *J Magn Magn Mater* 160:98–101
4. Netto PGQ, Tavares RP, Isac M, Guthrie RIL (2001) A technique for the evaluation of instantaneous heat fluxes for the horizontal strip casting of aluminum alloys. *ISIJ Int* 41(11):1340–1349
5. Luiten EEM, Blok K (2003) Stimulating R&D of industrial energy-efficient technology; the effect of government intervention on the development of strip casting technology. *Energy Policy* 31(13):1339–1356
6. Park JY, Oh KH, Ra HY (2001) The effects of superheating on texture and microstructure of Fe-4.5 wt% Si steel strip by twin-roll strip casting. *ISIJ Int* 41:70–75
7. Park JY, Oh KH, Ra HY (1999) Microstructure and crystallographic texture of strip-cast 4.3 wt% Si steel sheet. *Scr Mater* 40:881–885
8. Honma H, Ushigami Y, Suga Y (1991) Magnetic properties of (110)[001] grain oriented 6.5% silicon steel. *J Appl Phys* 70:6259–6261
9. Loulou T, Artyukhin EA, Bardon JP (1999) Estimation of thermal contact resistance during the first stages of metal solidification process: I—experiment principle and modelisation. *Int J Heat Mass Tran* 42(12):2129–2142
10. Nolli P, Cramb AW (2008) Naturally deposited oxide films in near-net-shape casting: importance, mechanisms of formation, and prediction. *Metall Mater Trans, B* 39(B):56–65
11. Nolli P, Cramb AW (2007) Interaction between iron droplets and H_2S during solidification. *ISIJ Int* 47:1284–1293
12. Yu Y, Cramb AW, Heard R, Fang Y, Cui J (2006) The effect of oxygen partial pressure on heat transfer and solidification. *ISIJ Int* 46(10):1427–1431
13. Zhu CY, Wang WL, Lu C (2019) Characterization of cermet coatings and its effect on the responding heat transfer performance in strip casting process. *J Alloy Compd* 770:631–639

14. Wang WL, Zhu CY, Lu C, Yu J, Zhou LJ (2018) Study of the heat transfer behavior and naturally deposited films in strip casting by using droplet solidification technique. *Metall Mater Trans, A*
15. Strezov L, Herbertson J (1998) Experimental studies of interfacial heat transfer and initial solidification pertinent to strip casting. *ISIJ Int* 38:959–966
16. Strezov L, Herbertson J, Belton GR (2000) Mechanisms of initial melt/substrate heat transfer pertinent to strip casting. *Metall Mater Trans, B* 31(B):1023–1030
17. Jenkins K, Lindenmo M (2008) Precipitates in electrical steels. *J Magn Magn Mater* 320:2423–2429
18. Iwayama K, Haratani T (1980) The dissolution and precipitation behavior of Mn and MnS in grain-oriented 3% silicon-steel with high permeability. *J Magn Magn Mater* 19:15–17
19. Fabrício Luiz de ALCÂNTARA (2013) Aluminium nitride precipitation in Fe-3% Si Steel. *ISIJ Int* 53:1211–1214
20. Wriedt HA, Hsun HU (1976) The solubility product of manganese sulfide in 3 pct silicon-iron at 1270 to 1670 K. *Metall Mater Transactions, A*, 7(4):711–718